Explicit Coherence Enhancing Filter With Spatial Adaptive Elliptical Kernel

Fang Li, Ling Pi, and Tieyong Zeng

***Abstract*—The goal of this letter is to provide an elliptical filter to improve image coherence for the task of image smoothing and inpainting. The kernel of this filter is adaptively weighted and its shape is determined by local coherence estimation. The long axis of its ellipse is the same as the coherence direction and we put more weight there to enhance coherence. Compared with the related anisotropic partial differential equations (PDEs) or wavelet shrinkage methods, the proposed filter is extremely simple, instinctive and easy to code. Numerical examples and comparisons illustrate clearly the good performance of the proposed filter.**

***Index Terms*—Coherence, elliptical kernel, inpainting, structure tensor.**

I. Introduction

MANY applications in image processing and computer vision involve the concept of image filtering since it can readily reduce noise or extract image features. The basic idea of explicit image filter is as follows: Assume that the input two-dimensional image is $u(x)$ defined on the grid $\Omega = \{1,\ldots,n\} \times \{1,\ldots,n\}$, and the weight kernel at x with respect to its neighboring position y is $w(x,y)$. Then the filtered output at x is given by:

$$v(x) = \sum_y w(x,y)u(y).$$

Evidently, the most important issue here is to design some suitable weight kernel $w(x,y)$ for different image processing tasks. In literature, the existing image filters in the space domain can be roughly classified into three types: linear spatial filter, spatial and range filter, or guided filter. The weight kernel of the first type is spatially invariant and independent of image content, typically we have: mean filter, Gaussian filter, Laplacian filter, Sobel filter etc [15]. And oriented filter, such as the classical steerable filters [13] and Gabor filter [14], is typical instance of spatial filter whose weight kernel depends on orientation. The second type is slightly different as its kernel weight $w(x,y)$ is related to x, y and $u(x), u(y)$. Typical examples are the Susan filter [17], the popular bilateral filter for edge-preserving smoothing [12], [18], and the nonlocal mean filter which is useful for texture image denoising [5]. The third type, the guided filter, is further different as its weight kernel is calculated according to another guiding image which may be different from the input image [16].

Similar to edges and textures, coherence is another important image feature. Roughly speaking, coherence measures the directional flow information in images. The exact definition of coherence is given by a mathematical formula based on structure tensor addressed in Section II. Intuitively, edges, lines and flow like structures have higher coherence than other structures. So keeping and enhancing the coherence is important in many image processing tasks. The classical method to enhance coherence is via anisotropic diffusion proposed by Weickert [19]–[21]. Besides image smoothing/denosing problems, the anisotropic diffusion methods are widely studied in image inpainting problems [2], [8]–[10]. Anisotropic diffusion requires sophisticated numerical methods [11], [21]. The idea of anisotropic diffusion is generalized to Harr wavelet framework and applied in image inpainting problems in [6], [7]. Image inpainting methods based on coherence transport are studied in [3], [4] where the inpainting pixels need to be serialized and fast marching technique is involved in the numerical implementation.

In this letter, we propose an explicit filter for image coherence enhancing. Our basic idea is: in order to design a weight kernel centered at some pixel with high coherence, more weight should be placed along the coherence direction and much less on the perpendicular direction. This motivates us to design an elliptical kernel whose long axis coincides with the coherence direction. The proposed filter has a more intuitive explanation than the related anisotropic diffusion PDE and the anisotropic wavelet shrinkage. Moreover, the proposed kernel itself is also new. Experiments in image smoothing and image inpainting demonstrate the effectiveness of the proposed filter. The letter is organized as follows. In Section II, we give the definition of coherence and methods to estimate it. Then we propose the new filter in Section III. The numerical experiments are displayed in Section IV. Finally, we conclude the letter in Section V.

II. Coherence Estimation

To define the coherence, we need go back to the concept of nonlinear structure tensor [1], [19], [22] which is used to extract

Manuscript received April 12, 2012; revised June 16, 2012; accepted June 24, 2012. Date of publication June 28, 2012; date of current version July 11, 2012. This work was supported by the 973 Program (2011CB707104), the National Science Foundation of China (11001082, 10901104, 10871126), and RGC 211710, 211911 and RFGs of HKBU. The associate editor coordinating the review of this manuscript and approving it for publication was Prof. Ce Zhu.

F. Li is with the Department of Mathematics, East China Normal University Shanghai 200241, China (e-mail: fli@math.ecnu.edu.cn).

L. Pi is with the Department of Mathematics, Shanghai Jiao Tong University, Shanghai 200240, China (e-mail: piling2007@gmail.com).

T. Zeng is with Department of Mathematics, Hong Kong Baptist University, Kowloon Tong, Hong Kong, China (e-mail: zeng@hkbu.edu.hk).

Color versions of one or more of the figures in this paper are available online at http://ieeexplore.ieee.org.

Digital Object Identifier 10.1109/LSP.2012.2206582

local image features. Assume that $u(x): \Omega \to \mathbb{R}$ is the observed image. Similar to [19], to avoid false detections due to noise, u is convolved with a Gaussian kernel G_σ: $u_\sigma = G_\sigma * u$. Denote:

$$\nabla u_\sigma \nabla u_\sigma^T := \begin{pmatrix} (u_\sigma)_{x_1}^2 & (u_\sigma)_{x_1}(u_\sigma)_{x_2} \\ (u_\sigma)_{x_1}(u_\sigma)_{x_2} & (u_\sigma)_{x_2}^2 \end{pmatrix},$$

where $x = (x_1, x_2)$ and $(u_\sigma)_{x_i}$ represents the partial derivative of u_σ with respect to x_i, $i = 1, 2$. The structure tensor is then defined as the matrix (see [19]):

$$J_\rho(\nabla u_\sigma) = G_\rho * (\nabla u_\sigma \nabla u_\sigma^T),$$

where G_ρ is convolved with each component of the matrix $\nabla u_\sigma \nabla u_\sigma^T$. The eigenvalues of the matrix $J_\rho(\nabla u_\sigma)$ are given by (see [1]):

$$\begin{cases} \mu_1 = \frac{1}{2}\left(J_{11} + J_{22} + \sqrt{(J_{11} - J_{22})^2 + 4J_{12}^2}\right), \\ \mu_2 = \frac{1}{2}\left(J_{11} + J_{22} - \sqrt{(J_{11} - J_{22})^2 + 4J_{12}^2}\right), \end{cases}$$

where J_{lk} are the elements of $J_\rho(\nabla u_\sigma)$. Evidently $\mu_1 \geq \mu_2$. The corresponding eigenvectors are parallel to:

$$\begin{cases} v_1 = \begin{pmatrix} 2J_{12} \\ J_{22} - J_{11} + \sqrt{(J_{11} - J_{22})^2 + 4J_{12}^2} \end{pmatrix}, \\ v_2 = v_1^\perp. \end{cases}$$

Let us denote the normalized vector of v_1 as $(\cos\theta, \sin\theta)$, i.e., the angle of v_1 and the positive direction of horizontal axis is θ. The vector v_1 indicates the orientation maximizing the gray-value fluctuations, while $v_1^\perp$ is vector perpendicular to v_1. The eigenvalues μ_1, μ_2 convey shape information. Indeed, typically, isotropic structures are characterized by $\mu_1 \cong \mu_2$; linelike structures imply $\mu_1 \gg \mu_2 \approx 0$; and corners mean $\mu_1 \geq \mu_2 \gg 0$. The coherence is then defined by $(\mu_1 - \mu_2)^2$ and the coherence direction is regarded as along v_2 (see [1]).

The steerable filters [13] are also extremely useful to extract the local dominant orientation. The oriented energy using second order steerable filters there is:

$$\begin{aligned} &E_2(\alpha) \\ &= C_1 + C_2\cos(2\alpha) + C_3\sin(2\alpha) + [\text{higher order terms} \cdots], \end{aligned}$$

where C_1, C_2, C_3 are given in [13, Table 11]. Define:

$$\alpha_d := \frac{\arg[C_2, C_3]}{2}, \ \ S := \sqrt{C_2^2 + C_3^2}. \tag{1}$$

Then the role of the dominant orientation α_d is similar to the orientation θ defined by structure tensor, and the length S is similar to $|\mu_1 - \mu_2|$.

III. The Proposed Filter

In this section, we will propose an explicit coherence enhancing filter which has a spatial adaptive elliptical kernel. Our basic idea is that for a weight kernel centered at pixel x with high coherence, more weight should be placed along the coherence direction, comparing with the perpendicular direction. This motivates us to design an elliptical kernel whose long axis coincides with the coherence direction. Meanwhile, in the pixels without high coherence structure such as flat regions, the kernel should be similar to a gaussian circular kernel.

Let $x = (x_1, x_2) \in \Omega$ be the center of a window, and $y = (y_1, y_2)$ be a pixel in the window. The notation of structure tensor and the related quantities $\mu_1, \mu_2, v_1, v_2, \theta$ follow Section II. Let us define the weight kernel at x with respect to neighboring position y as:

$$w(x, y) = \frac{1}{2\pi\sigma_1\sigma_2}\exp\left(-\frac{s'^2}{2\sigma_1^2} - \frac{t'^2}{2\sigma_2^2}\right), \tag{2}$$

where

$$\begin{cases} s' = (y_1 - x_1)\cos\theta + (y_2 - x_2)\sin\theta, \\ t' = -(y_1 - x_1)\sin\theta + (y_2 - x_2)\cos\theta, \end{cases} \tag{3}$$

and

$$\begin{cases} \sigma_1 = 10\gamma, \\ \sigma_2 = 10\left(\gamma + (1 - \gamma)\exp\left(\frac{-1}{(\mu_1 - \mu_2)^2 + \epsilon}\right)\right), \end{cases} \tag{4}$$

where γ is a small positive parameter and ϵ is very small positive number used to avoid dividing by zero.

Let us give some explanation of the above construction of the kernel $w(x, y)$. Note that the shape:

$$\frac{1}{2\pi\sigma_1\sigma_2}\exp\left(-\frac{s^2}{2\sigma_1^2} - \frac{t^2}{2\sigma_2^2}\right), \tag{5}$$

with $s = y_1 - x_1, t = y_2 - x_2$ is a standard ellipse centered at x with horizontal and vertical axis, see the blue kernel in Fig. 1. By rotation transform in (3), the horizontal axis of the ellipse is rotated to direction v_1, and the vertical axis is rotated to the coherence direction v_2, see the red ellipse in Fig. 1. Since we want more weight along the coherence direction for high coherence structures, we should choose σ_2 bigger than σ_1 and at the same time σ_2 increases with coherence. This motivates the choice of σ_1, σ_2 in (4). For isotropic structure, as $\mu_1 \approx \mu_2$, we have:

$$\sigma_2 \approx \sigma_1,$$

which gives isotropic weight kernel. For high coherence structures such as lines and edges, we have:

$$\sigma_1 = 10\gamma < \sigma_2 \in (10\gamma, 10),$$

since γ is very small, and σ_2 increases with the coherence $(\mu_1 - \mu_2)^2$. This results in anisotropic elliptical weight kernel and more weight is placed along the coherence direction v_2. By this we enhance the coherence.

The kernel can be easily generalized to color image case [20]. Assume that $\mathbf{u}(x) = (u^1, u^2, u^3): \Omega \to \mathbb{R}^3$ is the observed image. Each component $\mathbf{u}^j$, $j = 1$ to 3, is convolved with a Gaussian kernel G_σ and we get $u_\sigma^j = G_\sigma * u^j$. The structure tensor for color image is a natural generalization of the gray scale image case:

$$J_\rho(\nabla \mathbf{u}_\sigma) = G_\rho * \begin{pmatrix} \sum_j (u_\sigma^j)_{x_1}^2 & \sum_{j,k} (u_\sigma^j)_{x_1}(u_\sigma^k)_{x_2} \\ \sum_{j,k} (u_\sigma^j)_{x_1}(u_\sigma^k)_{x_2} & \sum_j (u_\sigma^j)_{x_2}^2 \end{pmatrix}.$$

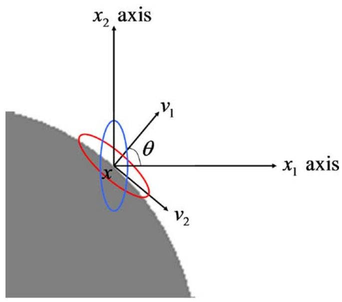

Fig. 1. The sketch map of elliptical kernel at x. v_1, v_2 and θ are as defined in Section II. The blue ellipse displays a level set of the kernel (5), and the red ellipse displays the level set of the rotated kernel (2).

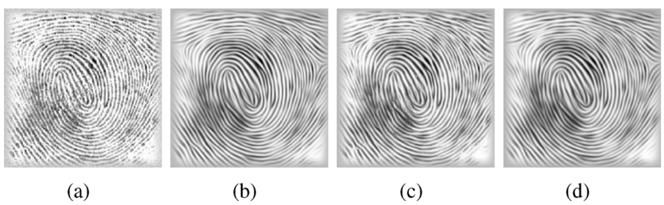

Fig. 2. Image smoothing. (a) Noisy fingerprint image; (b) result of anisotropic PDE diffusion method in [19]; (c) result of the proposed filter with coherence estimated by steerable filters. (d) result of the proposed filter with coherence estimated by structure tensor.

Then the coherence information can be extracted as in the gray image case. Using this structure tensor to define coherence is better than channel by channel method since the three channels are combined together.

Interestingly, we can use α_d and S in (1) estimated by steerable filters to substitute θ in (3) and $|\mu_1 - \mu_2|$ in (4) in the above framework respectively to construct another special filter. Numerically, we observe that our filter with coherence estimated by structure tensor has better performance for image smoothing (see Fig. 2 and discussion below).

Indeed, the proposed elliptical filter is adaptive to the task of image smoothing and inpainting for images with some high coherence features. The filter can be applied many times before getting a satisfying result, especially for image inpainting problems.

IV. Numerical Results

In this section, we report some experiments on gray/color image smoothing and inpainting with the proposed filter. Note that for our explicit filter, the filtered output at a pixel x is given by the summation of the image and the weight kernel in a local window centered at x. In all the experiments, the default values of parameters are: $\sigma = 1, \rho = 3, \gamma = 0.05, \epsilon = 2.2204 \times 10^{-16}$ (This is constant "eps" in MATLAB), the window size of structure tensor is $\lceil 3\sigma \rceil \times \lceil 3\sigma \rceil$ where $\lceil \cdot \rceil$ is the classical ceiling function, and the window size of the proposed kernel is 11×11. The central difference scheme is used in calculating all the gradient in structure tensor. For image inpainting, the initial value is taken as the input image with mask filled by random values. In all the experiments, we use structure tensor as the default method to estimate the coherence due to its simplicity and effectiveness.

In terms of computational efficiency, the proposed filter takes about 1 to 1.1 seconds on a 256×256 image when applying once (under Windows 7 and MATLAB v7.4 with Intel Core i5 M450 CPU and 2 GB memory).

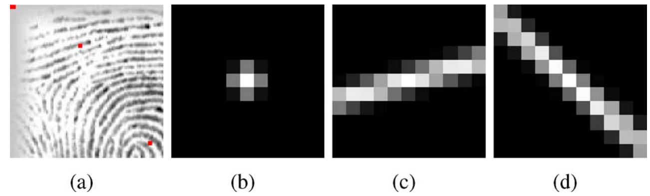

Fig. 3. The shape of the kernels at different pixels. (a) Upper left part of the fingerprint image in Fig. 2(a) with three red masks cover pixels (1,1), (30,50) and (100,100); (b)-(d) kernels at pixels (1,1), (30,50) and (100,100) respectively.

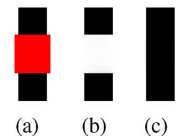

Fig. 4. Gray image inpainting. (a) Image with inpainting region marked by red color; (b) result of TV inpainitng; (c) result of the proposed Filter 1, filtering 200 times.

A. Coherence Enhancing Smoothing

In Fig. 2, we test a fingerprint image where the flow like structure is dominant. Fig. 2(a) is the test image. Fig. 2(c) shows the result of the proposed filter in which the coherence is estimated by steerable filters, while Fig. 2(d) shows the result of the proposed filter in which the coherence is estimated by structure tensor. The result Fig. 2(d) seems comparable with the result by the anisotropic PDE method in [19] shown in Fig. 2(b). The result Fig. 2(c) seems not so good as Fig. 2(b) and (d).

In Fig. 3, we display the kernels at three representative pixels in the fingerprint image tested in Fig. 3. The red square in Fig. 3(a) marked the choosing pixels (1,1), (30,50) and (100,100). Pixel (1,1) is isotropic structure as displayed in Fig. 3(b). Pixels (30,50) and (100,100) have line structure along different coherence directions, see Fig. 3(c)-(d) for the elliptical shape of kernels.

B. Image Inpainting

The proposed filter can be used in image inpainting by applying the filter many times. In the following, we compare our method with some other popular variational inpainting methods including total variation (TV) inpainting method in [8] and frame based inpainting method in [6], [7].

In Fig. 4, a bar image is tested. The red mask in Fig. 4(a) indicates the inpainting region where information is lost. The TV model broken the bar since in that way the TV norm attains its minimum, see Fig. 4(b). While the proposed filter can complete the bar in Fig. 4(c).

In Fig. 5, we compare the proposed filter with some other inpainting methods. Fig. 5(a) is the ground truth image. In Fig. 5(b) the red masks indicate the inpainting regions. Fig. 5(c) shows the result of cubic interpolation method by MATLAB routine "griddata". Fig. 5(d) shows the result of frame shrinkage method in [6]. The result of anisotropic harr wavelet shrinkage [7] is displayed in Fig. 5(e). The last one Fig. 5(f) is the result of our proposed filter. The peak signal-to-noise ratio (PSNR) is reported to compare the performance of each method. Our result is about 2.5 dB higher than the state of the art in Fig. 5(e).

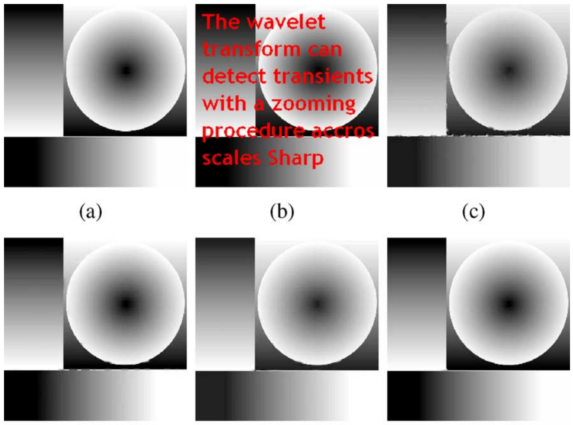

(a) (b) (c)

(d) (e) (f)

Fig. 5. Gray image inpainting. (a) The true image; (b) image with mask marked by red words; (c) cubic interpolation, $\mathrm{PSNR} = 29.39$ dB; (d) result of the frame inpainting method in [6], $\mathrm{PSNR} = 33.27$ dB; (e) result of anisotropic harr wavelet inpainting method in [7], $\mathrm{PSNR} = 38.58$ dB; (f) result of the proposed spatial elliptical filter, filtering 280 times, $\mathrm{PSNR} = 41.00$ dB.

(a) (b) (c)

(d) (e) (f)

Fig. 6. Color image inpainting. (a) Image with mask marked by red words; (b) result of TV inpainitng; (c) result of the proposed filter, filtering 80 times, $\rho = 6$, window size is 7×7; (d)-(f) zoomed small subregions (indicated by yellow rectangle in (a)) of the images in (a)-(c) for detail comparison.

It is clear that the edge of the big circle and the horizontal line below are better recovered. We remark that in this example, we set $\sigma = 0$ which means that $u_\sigma^j = u^j$, $j = 1, 2, 3$, and update $\gamma = \gamma/1.6$ every 40 filtering iterations beginning with $\gamma = 0.05$. The reason of reducing γ gradually is: in the proposed filter a smaller γ favors more coherence, but if we set γ too small at the beginning, the error information in the inpainting domain will lead to wrong estimation of coherence direction and lead to bad results. Remark that Fig. 5(c)–(e) are taken from [7].

In Fig. 6, a color image with red word masks indicating the inpainting regions is tested. Fig. 6(b) and (c) display the inpainting results of TV model and the proposed filter respectively. To see the advantage of the proposed method, a small subregion is zoomed in the second row for detail comparison. It is shown that the proposed filter can better recover the coherence of the eave.

V. Conclusion

The novelty of the letter is the designing of spatial adaptive elliptical kernel. We determine the shape of the elliptical kernel by coherence estimation. The long axis of the corresponding ellipse coincides with the coherence direction such that more weight is placed on this direction, and then the coherence can be enhanced. The proposed filter is extremely simple but effective for important image processing tasks such as image smoothing and image inpainting. Following the similar idea in this letter, one can design other type anisotropic kernel according to some geometrical cues in images. Mathematically, the proposed filter should be related to some minimization problem. This will be our future work.

Acknowledgment

The authors would like to thank J.-F. Cai for providing the test image and mask in Fig. 5. They also thank the anonymous reviewers for the extremely helpful comments.

References

[1] G. Aubert and P. Kornprobst, *Mathematical Problems in Image Processing: Partial Differential Equations and the Calculus of Variations (Applied Mathematical Sciences)*, 2nd ed. Berlin, Germany: Springer-Verlag, 2006.

[2] C. Ballester, M. Bertalmío, V. Caselles, G. Sapiro, and J. Verdera, "Filling-in by joint interpolation of vector fields and gray levels," *IEEE Trans. Image Process.*, vol. 10, pp. 1200–1211, 2001.

[3] F. Bornemann and T. März, "Fast image inpainting based on coherence transport," *J. Math. Imag. Vis.*, vol. 28, no. 3, pp. 259–278, 2007.

[4] T. März, "Image inpainting based on coherence transport with adapted distance functions," *SIAM J. Imag. Sci.*, vol. 4, no. 4, pp. 981–1000.

[5] A. Buades, B. Coll, and J. M. Morel, "A review of image denoising algorithms, with a new one," *Multiscale Model. SIM*, vol. 4, no. 2, pp. 490–530, 2005.

[6] J. Cai, R. Chan, and Z. Shen, "A framelet-based image inpainting algorithm," *Appl. Comput. Harmon. Anal.*, vol. 24, no. 2, pp. 131–149, 2008.

[7] R. Chan, S. Setzer, and G. Steidl, "Inpainting by flexible Haar-wavelet shrinkage," *SIAM J. Imag. Sci.*, vol. 1, no. 3, pp. 273–293, 2008.

[8] T. Chan and J. Shen, "Mathematical models for local nontexture inpaintings," *SIAM J. Appl. Math.*, vol. 62, pp. 1019–1043, 2002.

[9] T. Chan and J. Shen, "Non-texture inpainting by curvature-driven diffusion (CDD)," *J. Vis. Commun. Image Represent.*, vol. 12, pp. 436–449, 2001.

[10] T. Chan, S. Kang, and J. Shen, "Euler's elastica and curvature based inpainting," *SIAM J. Appl. Math.*, vol. 63, pp. 564–592, 2002.

[11] Y. Chen and S. Levine, "Image recovery via diffusion tensor and time-delay regularization," *J. Vis. Commun. Image Represent.*, vol. 13, no. 1, pp. 156–175, 2002.

[12] M. Elad, "On the origin of the bilateral filter and ways to improve it," *IEEE Trans. Image Process.*, vol. 11, no. 10, pp. 1141–1151, 2002.

[13] W. T. Freeman and E. H. Adelson, "The design and use of steerable filters," *IEEE Trans. Patt. Anal. Mach. Intell.*, vol. 13, no. 9, pp. 891–906, 1991.

[14] D. Gabor, "Theory of communication," *J. IEEE*, vol. 93, pp. 429–459, 1946.

[15] R. C. Gonzalez and R. E. Woods, *Digital Image Processing*, 3rd ed. Upper Saddle River, NJ: Prentice-Hall, 2007.

[16] K. He, J. Sun, and X. Tang, "Guided image filtering," in *The 11th Eur. Conf. Computer Vision (ECCV 2010)*, 2010.

[17] S. M. Smith and J. M. Brady, "Susan – A new approach to low level image processing," *Int. J. Comput. Vis.*, vol. 23, no. 1, pp. 45–78, 1997.

[18] C. Tomasi and R. Manduchi, "Bilateral filtering for gray and color images," in *Sixth Int. Conf. Computer Vision*, 1998, pp. 839–846.

[19] J. Weickert, "Coherence-enhancing diffusion filtering," *Int. J. Comput. Vis.*, vol. 31, no. 2/3, pp. 111–127, 1999.

[20] J. Weickert, "Coherence-enhancing diffusion of colour images," *Image Vis. Comput.*, vol. 17, pp. 201–212, 1999.

[21] J. Weickert and H. Scharr, "A scheme for coherence-enhancing diffusion filtering with optimized rotation invariance," *J. Vis. Commun. Image Represent.*, vol. 13, no. 1/2, pp. 103–118, 2002.

[22] J. Weickert and T. Brox, "Diffusion and regularization of vector- and matrix-valued images," in *Inverse Problems, Image Analysis, and Medical Imaging*, M. Z. Nashed and O. Scherzer, Eds. Providence, RI: AMS, 2002, vol. 313, Contemporary Mathematics, pp. 251–268.